Acta Cryst. (1995). B**51**, 604–618

Structural Aspects of Superconducting Cuprates

BY C. N. R. RAO*

Solid State and Structural Chemistry Unit, Indian Institute of Science, Bangalore 560 012, *India, and Department of Chemistry, University of Wales, Cardiff CF*1 3*TB, Wales*

AND A. K. GANGULI

CSIR Centre of Excellence in Chemistry, Indian Institute of Science, Bangalore 560 012, *India*

(*Received* 11 *August* 1994; *accepted* 15 *December* 1994)

Abstract

Salient structural features of the important families of cuprate superconductors are briefly reviewed. Correlations between the superconducting transition temperature and some of the crucial structure parameters are discussed. Correlations include those with the in-plane Cu—O distances, apical Cu—O distance, Madelung potentials and bond valence sums. The transformation of $YBa_2Cu_3O_{6.7}$ (123 cuprate) to a $YBa_2Cu_4O_8$ (124)-type phase is examined. Structural features of the newly discovered oxyanion derivatives of cuprates are pointed out.

1. Introduction

Superconductivity is an old phenomenon. Many types of superconducting materials have been investigated over the past several decades. These include metals, alloys, metal oxides and organic materials. In spite of these efforts the highest superconducting transition temperature achieved until 1986 was 23 K in alloys of niobium. Oxides such as $BaPb_{1-x}Bi_xO_3$ and $LiTi_2O_4$ had transition temperatures of ~13 K. The discovery of superconductivity around 30 K in the La–Ba–Cu–O family (Bednorz & Müller, 1986) completely changed the situation. Since then a variety of cuprate superconductors with transition temperatures up to 150 K have been synthesized and characterized (Rao, 1991*a*; Raveau, Michel, Hervieu & Groult, 1991; Nunez-Regueiro, Tholence, Antipov, Capponi & Marezio, 1993). The structures of these materials have been extensively investigated by X-ray and neutron diffraction techniques (especially powder profile analysis) and high-resolution electron microscopy. Although no simple relation exists between superconductivity and the structure of the cuprates, it has been possible to relate superconductivity with some of the structural parameters and identify important commonalities. These correlations help to understand the nature of cuprate materials and to design new materials. We describe herein the structural features of some of the families of cuprates and review the important structure–property relations in superconducting cuprates. We also examine certain interesting structural aspects of the transformation of oxygen-deficient 123 cuprates, as well as of the recently discovered oxyanion derivatives of cuprates.

* Author to whom correspondence should be addressed at: The Solid State and Structural Chemistry Unit, Indian Institute of Science, Bangalore 560012, India.

2. Structural features of some of the cuprate families

We shall briefly examine the salient structural aspects of the major types of cuprate superconductor.

2.1. $La_{2-x}A_xCuO_4$ (A = Ca, Sr, Ba)

Cuprates of the general formula Ln_2CuO_4 (Ln = rare-earth metal) possess either the quasi-two-dimensional K_2NiF_4 (T) or the T' structure (Fig. 1), depending on the rare-earth containing CuO_6 octahedra and CuO_4 square planes, respectively. Both the T and T' structures crystallized in the $I4/mmm$ space group. The T^* structure (space group $P4/nmm$) containing CuO_5 square pyramids (Fig. 1) can be obtained by taking half the unit cell (along c) of T and T' and joining together. Matching between the Ln—O bond length and $2^{1/2}$ of the Cu—O bond length is of importance in understanding not only the T and T' structures, but also the orthorhombic distortion in La_2CuO_4 below 500 K. The tolerance factor t is a useful guide

$$t = (r_A + r_O)/2^{1/2}(r_B + r_O),$$

where r is the radius of the relevant ion. When $t \approx 1$, the bond-matching situation is ideal; when $t < 1$ (0.89 in La_2CuO_4) the Cu—O planes are under compression and the Ln—O bonds under tension. The different ways in which such a strained system can adjust to the mismatch are (Goodenough & Manthiram, 1991): (i) by a large c/a distortion, (ii) by creating an oxygen-rich phase such as $La_2CuO_{4+\delta}$, (iii) tetragonal–orthorhombic distortion and (iv) by a $T - T'$ transition (*e.g.* $La_{2-y}Nd_yCuO_4$). We see from the phase diagram in Fig. 2 that there is an intermediate phase T'' which has a very narrow phase

ISSN 0108-7681

width (around $y = 0.5$). The structure of the T'' phase appears to be close to that of the T' phase. La_2CuO_4 is itself orthorhombic (distorted T structure) and becomes superconducting ($T_c \sim 30$–40 K) when doped with excess oxygen. It has an interesting phase diagram (Dabrowski *et al.*, 1989; Jorgensen, 1991), with $La_2CuO_{4.03}$ showing phase separation at 320 K into stoichiometric La_2CuO_4, which is antiferromagnetic, and oxygen-excess $La_2CuO_{4.08}$, which is superconducting ($T_c \sim 40$ K).

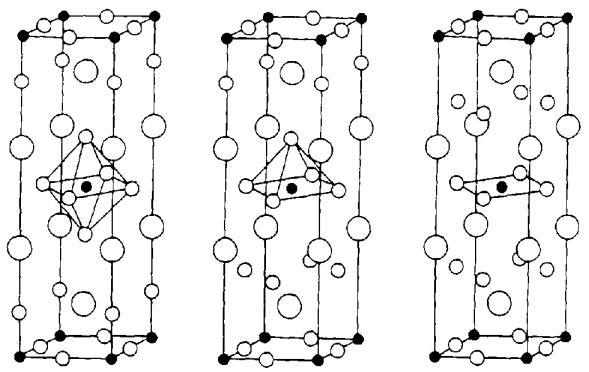

Fig. 1. T-, T^*- and T'-type tetragonal structures of Ln_2CuO_4-type compounds.

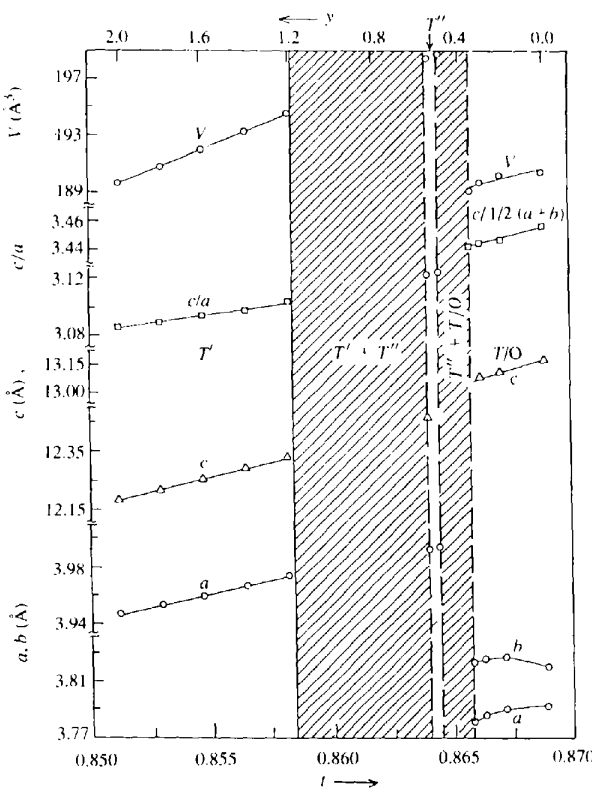

Fig. 2. Variation of the lattice parameters and volume with y in $La_{2-y}Nd_yCuO_4$, showing regions of T, T' and T'' structures [adapted from Goodenough & Manthiram (1991)].

On substituting La partly by an alkaline earth ion, as in $La_{2-x}A_xCuO_4$, the structure becomes tetragonal (T) with elongated CuO_6 octahedra (Fig. 1) having the space group $I4/mmm$ (Cava, Santoro, Johnson & Rhodes, 1987) at room temperature for $x > 0.05$ ($a \sim 3.8$, $c \sim 13.2$ Å). The structure becomes orthorhombic around 180 K, well above the superconducting transition (25–40 K). Sr_2CuO_3 which has a structure related to La_2CuO_4 is an insulator, but becomes superconducting on oxygen doping under pressure. More interestingly, the oxyfluoride $Sr_2CuO_2F_{2+\delta}$ with interstitial fluorines is superconducting (T_c, 46 K), the structure being close to that of $La_2CuO_{4+\delta}$ (Al-Mamouri, Edwards, Greaves & Slaski, 1994).

2.2. $LnBa_2Cu_3O_{7-\delta}$

The structure of these 123 cuprates is related to the ordered oxygen-deficient triple perovskite structure $(ABO_{3-\delta})_3$. The Ln and Ba atoms occupy the A sites in an ordered fashion with the B sites occupied by Cu. Both tetragonal and orthorhombic structures exist, depending on the oxygen content and the ordering (Fig. 3). Two-thirds of the Cu ions form CuO_2 planar sheets, derived from a square-pyramidal coordination for Cu, while one-third of the Cu ions form one-dimensional chains of planar CuO_4 groups running along the b-axis. The CuO_2 sheets are separated by Y or Ln ions. Orthorhombic $YBa_2Cu_3O_{6.91}$ crystallizes in the $Pmmm$ space group with $a \simeq 3.823$, $b \simeq 3.886$ and $c \simeq 11.68$ Å (Williams *et al.*, 1988). The ordered orthorhombic compositions of $LnBa_2Cu_3O_{7-\delta}$ ($\delta \approx 0.0$) exhibit T_c of around 90 K and there is practically no change in T_c on changing the Ln ion.

Oxygen non-stoichiometry in 123 cuprates, especially $YBa_2Cu_3O_{7-\delta}$, has been investigated in great detail. Besides the fully ordered orthorhombic structures (space group $Pmmm$; $\delta < 0.2$), there are tetragonal structures (space group $P4/mmm$; $\delta = 1.0$) where no chain oxygens are present and δ in the $0.6 < x < 1.0$ range, where

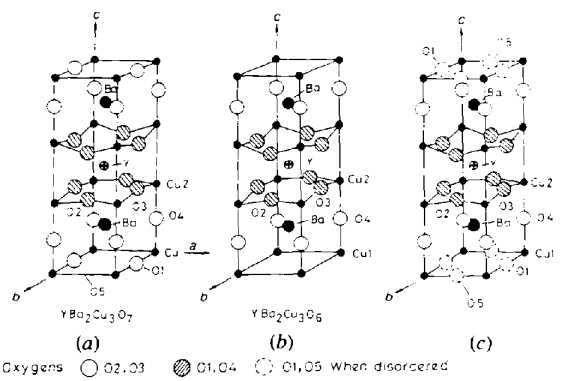

Fig. 3. Structures of $YBa_2Cu_3O_{7-\delta}$: (*a*) orthorhombic structure of the superconducting $\delta = 0.0$ phase; (*b*) tetragonal structure of the non-superconducting $\delta = 1.0$ phase with no Cu—O chain; (*c*) disordered structure of the tetragonal phase.

oxygen disorder in the basal plane leads to a tetragonal structure [Fig. 3(*c*)]. The plot of T_C against δ shows a plateau ($T_c \approx 60$ K) when $0.3 < \delta < 0.4$. The 60 K superconducting compositions do not appear to be genuinely stable phases, not being associated with well defined vacancy-ordered structures. Any oxygen added in this composition range oxidizes copper in the chains without affecting the hole concentration in the CuO_2 sheets. Well defined vacancy ordering is found (Rao, Nagarajan, Ganguli *et al.*, 1990) only when $\delta = 0.5$ and 0.25 rather than at $\delta = 0.0$ and 1.0, as shown in Fig. 4. The $2a_o \times b_o \times c_o$ structure ($\delta = 0.5$) is refered to as the *ortho*-II structure, the normal $a_o \times b_o \times c_o$ ($\delta < 0.2$) structure being the *ortho*-I structure. In the *ortho*-I regime ($\delta < 0.2$), one strictly observes that $c = 3b$. From Fig. 4(*c*), we see that the $\delta = 0.5$ composition is a recurrent intergrowth of the $\delta = 0.0$ and 1.0 compositions. X-ray diffraction studies on single crystals of $YBa_2Cu_3O_{7-\delta}$ show (Plakhty *et al.*, 1992) that the *ortho*-II phase exists in the range $0.40 < x < 0.63$. When δ is large ($\simeq 0.70$), the $3a_o \times b_o \times c_o$ superstructure has been found. There is some doubt regarding the superstructure of the $\delta = 0.25$ composition in Fig. 4(*b*).

All the orthorhombic 123 structures show twinning; $PrBa_2Cu_3O_{7-\delta}$ exhibits twinning although it is non-superconducting (Ganguli, Rao, Sequeira & Rajagopal, 1989), laying to rest an early speculation relating twinning and superconductivity. Twinning domains have been observed with a variety of spacings, the mean width being regular over a large area. Although X-ray diffraction studies may suggest a tetragonal phase, such twinned crystals may actually be orthorhombic.

$YBa_2Cu_4O_8$ (124), with $T_c = 80$ K, is structurally related to $YBa_2Cu_3O_7$. Instead of single CuO_4 linear chains (along the *b* axis) in the 123 structure, 124 cuprates have edge-shared CuO_4 units forming double chains (Fig. 5). They crystallize in the *Ammm* space group with $a \simeq 3.841$, $b \simeq 3.872$ and $c \simeq 27.24$ Å (Hewat *et al.*, 1990). Note that orthorhombic 123 crystallizes in the *Pmmm* structure with $a \simeq 3.823$, $b \simeq 3.886$, $c \simeq 11.680$ Å. 124 cuprates are stoichiometric with respect to oxygen and loss of oxygen occurs only at temperatures higher than 1100 K. $Y_2Ba_4Cu_7O_{15-\delta}$ (247), crystallizing in the orthorhombic structure (*Ammm*) with $a \simeq 3.85$, $b \simeq 3.87$ and $c \simeq 50.29$ Å (Bordet *et al.*, 1988), is an intergrowth of 123 and 124 slabs (Fig. 5). In the 247 cuprates, T_c varies as a function of oxygen content, with a maximum value of 92 K.

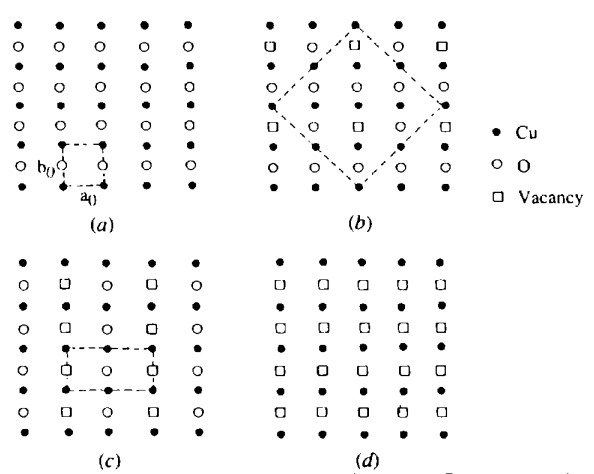

Fig. 4. Structure of the basal (*ab*) plane of $YBa_2Cu_3O_{7-\delta}$: (*a*) $\delta = 0.0$, (*b*) $\delta = 0.25$, (*c*) $\delta = 0.50$ and (*d*) $\delta = 1.0$ [from Rao (1991*b*)].

2.3. $Bi_2(Ca,Sr)_{n+1}Cu_nO_{2n+4}$

These cuprates have layered structures with two BiO rock-salt layers and $n(CuO_2)$ layers interleaved by Ca and Sr (Fig. 6). The two BiO layers are separated by a

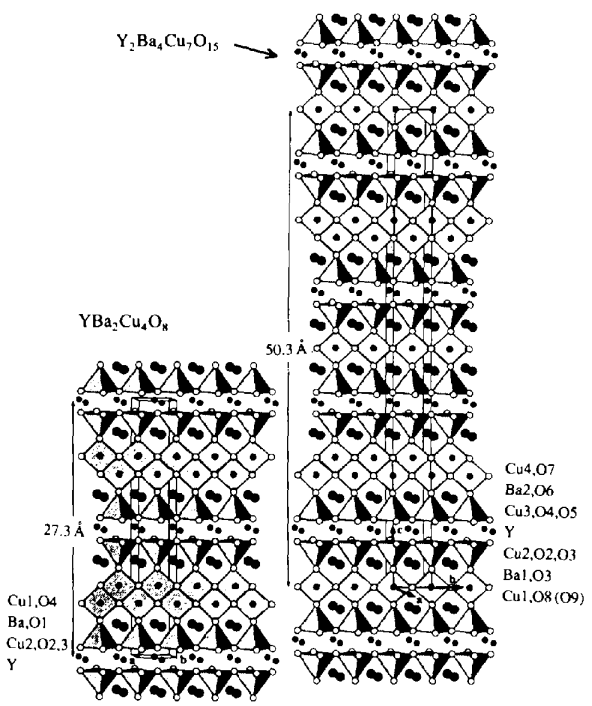

Fig. 5. Structures of $YBa_2Cu_4O_8$ and $Y_2Ba_4Cu_7O_{15}$.

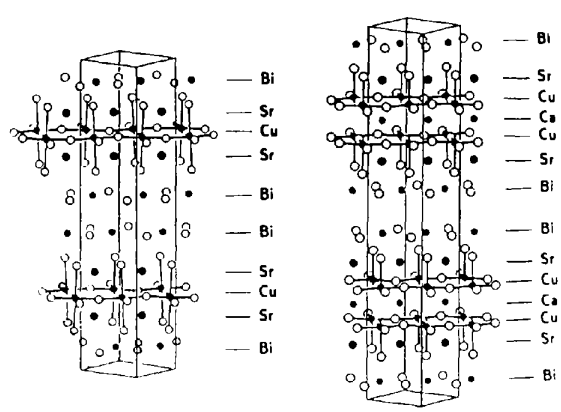

Fig. 6. Structures of $Bi_2(Ca,Sr)_{n+1}Cu_nO_{2n+4}$, with $n = 1$ and 2.

van der Waals gap of 3.2 Å. Since the Ca and Sr sites are interchangeable, the exact stoichiometry is rarely as per the general formula. The synthesis of the stoichiometric $n = 1$ phase poses some problems and T_c varies with the Bi/Sr ratio, the maximum value being 22 K. The stable $n = 2$ phase ($T_c \sim 90$ K) invariably forms to some extent (as an intergrowth) along with the $n = 1$ and 3 phases. The Bi cuprates crystallize in orthorhombic structures [space groups *Amaa* ($n = 1$), *A2aa* ($n = 2, 3$) with $a \simeq b \simeq 5.4$ Å and c varying from ~ 25 to ~ 36 Å for $n = 1$ and 3, respectively (Torardi, Parise, Subramanian, Gopalakrishnan & Sleight, 1989)]. An important structural feature of the Bi cuprates is the incommensurate modulation found along the b direction. Incommensurate modulation is also found in non-superconducting Bi cuprates such as $Bi_2YSr_2Cu_2O_8$ (Rao, Nagarajan, Vijayaraghavan *et al.*, 1990). Modulation-free superconductors have been synthesized, indicating that there is no relation between modulation and superconductivity in these cuprates (Manivannan, Gopalakrishnan & Rao, 1991).

2.4. *Thallium cuprates*

Structures of the $Tl_2Ca_{n-1}Ba_2Cu_nO_{2n+4}$ family of cuprates are similar to those of $Bi_2(Ca,Sr)_{n+1}Cu_nO_{2n+4}$ (Fig. 7). These cuprates have corner-sharing CuO_n ($n = 4, 5$ or 6) groups forming two-dimensional layers perpendicular to the c-axis (Torardi *et al.*, 1988). The separation between the Tl—O rock-salt layers is 2.2 Å. These double Tl—O layer cuprates have a tetragonal structure ($I4/mmm$) with the c parameter varying from 24 ($n = 1$) to 36 Å ($n = 3$), accompanying an increase in T_c from 90 ($n = 1$) to 125 K ($n = 3$).

Single Tl—O layer cuprates of the type $TlCa_{n-1}Ba_2Cu_nO_{2n+3}$ have the primitive tetragonal structure ($P4/mmm$), with the c-lattice parameters 9.0, 12.6 and 15.6 Å for $n = 1$, 2 and 3, respectively. The $n = 1$ member is semiconducting and is not easy to prepare in monophasic form; the $n = 2$ and 3 members are superconducting with T_c's of 90 and 115 K. There are

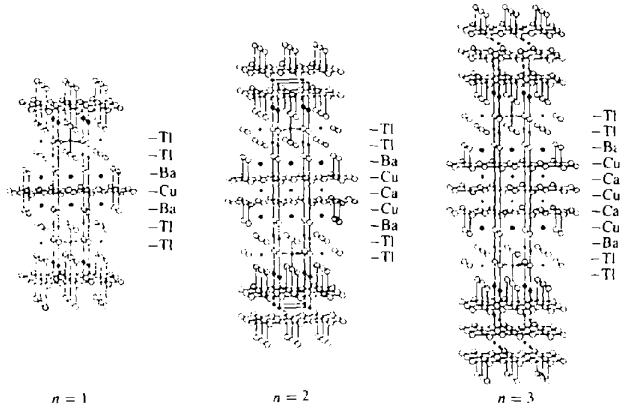

Fig. 7. Structures of the $n = 1$, 2 and 3 members of the $Tl_2Ca_{n-1}Ba_2Cu_nO_{2n+4}$ series.

no simple Sr analogues of the Ba-based Tl cuprates with one TlO layer. $TlSr_2CuO_5$ is difficult to synthesize in pure form. Partial substitution of Tl by Pb leads to stable compounds ($P4/mmm$) which are superconducting (Ganguli, Nanjundaswamy & Rao, 1988; Subramanian *et al.*, 1988). In the $Tl(Ca,Sr)_{n+1}Cu_nO_{2n+3}$ family of cuprates with one Tl—O layer, partial substitution of Ca or Sr by a rare earth also stabilizes the phases (Ganguli, Manivannan, Sood & Rao, 1989; Manivannan, Rangavittal, Gopalakrishnan & Rao 1993; Vijayaraghavan *et al.*, 1989).

2.5. *Lead-based superconductors*

$Pb_2Sr_2LnCu_3O_8$-type compounds become superconducting ($T_c \sim 70$ K) when Ln is substituted partly by Ca or Sr. These cuprates contain Cu^+ ions and are prepared in a reducing atmosphere to ensure that Pb is divalent. The compounds crystallize in an orthorhombic cell (*Cmmm*) with $a = 5.393$, $b = 5.431$ and $c = 15.733$ Å for $Pb_2Sr_2YCu_3O_8$ (Cava *et al.*, 1989). The structure (Fig. 8) comprises infinite CuO_2 sheets (copper is coordinated to five oxygens, forming a square pyramid) separated by Ln/Ca atoms. There is another CuO_δ layer (formally Cu^+) in which Cu is linearly coordinated to two O atoms. The Pb ions have a highly distorted square-pyramidal coordination, leading to an

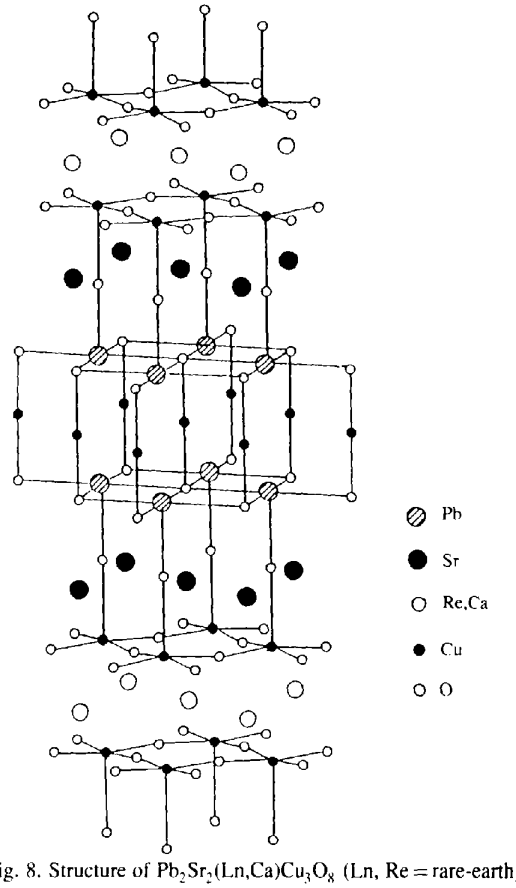

Fig. 8. Structure of $Pb_2Sr_2(Ln,Ca)Cu_3O_8$ (Ln, Re = rare-earth).

orthorhombic distortion. The structure can be compared with that of $Bi_2Sr_2CaCu_2O_{8+\delta}$ by replacing the PbO–CuO_δ–PbO triple layer with a $CuO_{1-\delta}$ layer and a BiO–BiO double layer.

Lead cuprates of the 0223 type (Fig. 9) with fluorite blocks ($PbBaSrY_{1-x}Ca_xCu_3O_y$; space group *I4/mmm*) have PbO–CuO_δ double layers rather than PbO–CuO_δ–PbO triple layers. Tl-based 1222 and 2222 cuprates and Bi-based 2222 cuprates as well as the Pb-based 0223 and 1222 cuprates possess fluorite layers in addition to the rock salt and perovskite-type layers, as shown in Fig. 9 (Kopnin, Kharlanov, Bryntse & Antipov, 1994). Typical compositions are $Tl_2Ba_2(Ln_{1-x}Ce_x)_2Cu_2O_{10+\delta}$ (2222), $Bi_2Sr_2(Ln,Ce)_2Cu_2O_{10+\delta}$ (2222), $(Pb,Cu)(Eu,Ce)_2$-$(Sr,Eu)_2Cu_2O_z$ (1222) ($T_c \sim 25$ K).

2.6. *Mercury cuprates*

Although 1212-type Hg cuprates related to Tl-based 1212 structures were synthesized some time ago, superconductivity was discovered in these materials only recently. $HgCa_{n-1}Ba_2Cu_nO_{2n+2}$ with $n = 1, 2, 3$ and 4 show T_c's of the order 95, 129, 133 and 126 K, respectively (Capponi *et al.*, 1993, and references therein). The $n = 3$ (1223) member has $T_c = 150$ K under high pressures [11–23.5 GPa (Nunez-Regueiro, Tholence, Antipov, Capponi & Marezio, 1993)]. This is the highest reproducible T_c reported for any superconductor so far. Structures of these superconductors are quite simple and are related to the single Tl—O layered cuprates (Fig. 10). The structures have *P4/mmm* space group, with $a \sim 3.85$ Å and a variable *c*-parameter depending on n [$c = 9.5 + (3.2)(n - 1)$ Å]. $HgBa_2$-$CuO_{4.065}$ has the highest T_c (95 K) of all cuprates with one Cu—O sheet, the excess oxygen being essential for hole-doping. Hg is almost two-coordinated forming O—Hg—O sticks along the *c*-axis. The excess oxygen enters in the Hg plane, giving HgO_δ with $\delta = 0.065$.

Hg^{2+} is different from Bi^{3+} and Pb^{2+} as it does not possess a lone pair of electrons. Hg^{2+} is, however, closer to Tl^{3+}. Accordingly, $HgCa_{n-1}Ba_2Cu_nO_{2n+2+\delta}$ compounds are indeed similar to $Tl_2Ca_{n-1}Ba_2Cu_nO_{2n+4+\delta}$. Hg^{2+} prefers a linear coordination in oxides. Thus, HgO has a chain structure where Hg is two-coordinated to oxygen in a linear fashion. Tl^{3+}, on the other hand, prefers an octahedral coordination. Due to this low coordination, a major structural difference between Hg-based superconductors and related Tl and Bi superconductors is the near absence of O atoms in the Hg planes. $HgBa_2CuO_{4+\delta}$ is not self-doped; $HgCa_2Ba_2Cu_3O_{8+\delta}$, however, is. In the analogous Tl_2 cuprates, the $n = 1, 2$ and 3 members are all self-doped. Why then do Hg cuprates have such high T_c's? What is the role of mercury? Or, what is special about mercury? These are some questions which need to be pondered over.

2.7. *Infinite-layer cuprates*

The first infinite-layer cuprate discovered, $Ca_{0.86}Sr_{0.14}CuO_2$ (Siegrist, Zahurak, Murphy & Roth, 1988), is not superconducting. Many simple layered superconductors in which the CuO_2 planes are infinitely stacked, separated by alkaline-earths (Fig. 11), have been characterized. Doping at the alkaline-earth site by a trivalent rare-earth is necessary for superconductivity in some cases, as exemplified by $Sr_{1-y}Ln_yCuO_2$ with T_c's of 40 K (Er, Miyamoto, Kanamaru & Kikkawa, 1991; Smith, Manthiram, Zhou, Goodenough & Markert, 1991). Cation vacancies (*e.g.* $Sr_{1-y}CuO_2$, $T_c \sim 70$–95 K) lead to superconductivity, while T_c's of the order 80–100 K have been attained by Takano, Azuma, Hiroi, Bando & Takeda (1991) in the Ba–Sr–Cu–O system, synthesized under high pressures. Azuma, Hiroi, Takano, Bando & Takeda (1992) report $T_c = 110$ K in $(Sr_{1-x}Ca_x)_{1-y}CuO_2$ ($0.3 \le x \le 0.6$, $y < 0.1$). This system is believed to have both electrons and holes,

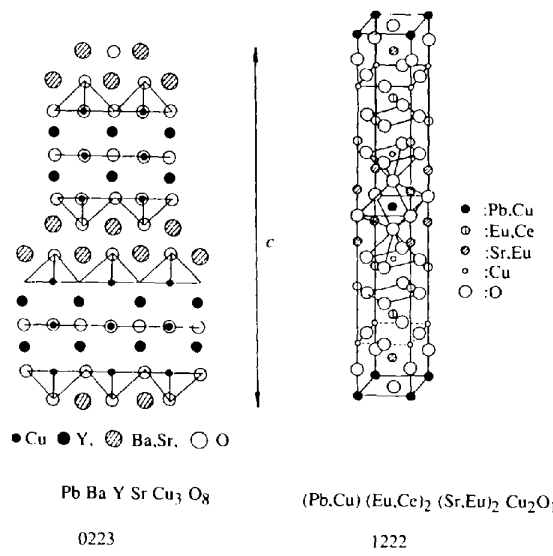

Fig. 9. Schematic structures of the fluorite-based 1222 and 0223 superconductors [from Kopnin, Kharlanov, Bryntse & Antipov (1994)].

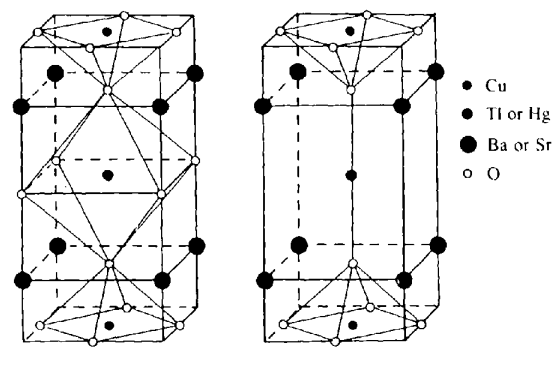

Fig. 10. Schematic structures of 1201-type Tl and Hg cuprates.

while $Sr_{1-y}Ln_yCuO_2$ (Ln = Ln, Pr, Nd) is an electron superconductor. High-resolution electron microscopy reveals the presence of several defect layers in $(Sr,Ca)_{1-y}CuO_2$. Recently these planar defects in $(Sr,Ca)CuO_2$ have been identified by quantitative X-ray and high-resolution electron microscopy (Zhang *et al.*, 1994). These authors propose that the defect consists of a corrugated Sr—O layer, substituting for a CuO_2 layer, with the incorporation of some apical oxygens (which are absent in the parent infinitely layered compound). This results in a Sr_3O_2 defect block intergrowing with the normal Sr, Ca–CuO_2–Sr, Ca layers. Such a defect model, where a variable apical oxygen content exists, can account for *n*- or *p*-type superconductivity, as well as non-superconducting properties. It is indeed known that these compounds show varying properties depending on whether high-pressure oxygenation, high-pressure reduction or high-pressure neutral-atmosphere annealing has been carried out on these materials.

2.8. *Electron superconducting cuprates*

Superconducting cuprates of the type $Ln_{2-x}A_xCuO_{4-\delta}$ (Ln = Nd, Pr, Sm, Eu and *A* = Ce or Th) have the *T'*–(Nd_2CuO_4) type structure (*I*4/*mmm*) shown in Fig. 1, made up of two-dimensional sheets of CuO_4 units perpendicular to the *c*-axis (Markert *et al.*, 1989; Tokura, Takagi & Uchida, 1989). The CuO_2 sheets in these cuprates are separated by fluorite-type $(Ln, Ln')_2O_2$ sheets. This structure is closely related to the *T* structure of Sr- or Ba-doped La_2CuO_4 (Fig. 1), in which Cu has an elongated octahedral coordination separated by rock-salt type Ln—O layers. Instead of hole-doping into square-pyramidal Cu in the hole superconductors, superconductivity in the *T'* structures is caused by electron-doping into the square-planar CuO_4 sheets by higher-valent rare-earth ions (Ce^{4+}, Th^{4+}) or by partially replacing O by F as in $Nd_2CuO_{4-x}F_x$ (James, Zahurak & Murphy, 1989). As mentioned earlier $Sr_{1-y}Ln_yCuO_2$ is also an electron superconductor.

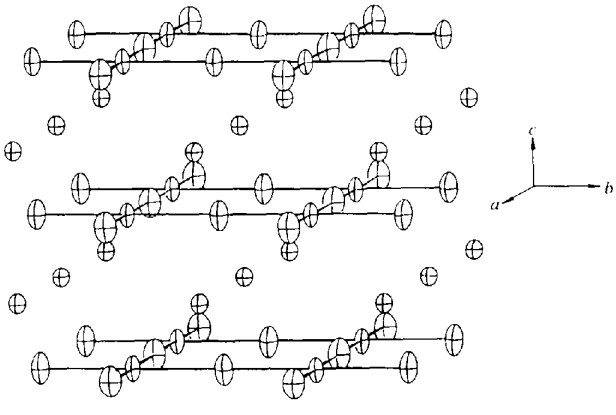

Fig. 11. Structure of $Ca_{0.86}Sr_{0.14}CuO_2$ having planar CuO_2 sheets separated by Ca, Sr [from Siegrist, Zahurak, Murphy & Roth (1988)].

3. Alternative representation of cuprate structures

The copper–oxygen framework is closely related to the perovskite structure in almost all the cuprate superconductors. Thus, $La_{2-x}(Ca,Sr,Ba)_xCuO_4$, as well as the Bi–Ca–Sr–Cu–O and Tl–Ca–Ba–Cu–O cuprates can be considered to belong to the same structural family involving the intergrowth of multiple oxygen-deficient perovskite layers $ACuO_{3-x}$, with rock-salt layers *AO* leading to the general formula $[ACuO_{3-x}]_n[AO]_n$ (Rao & Raveau, 1989). Based on this fomulation, $La_{2-x}M_xCuO_4$, $Bi_2Sr_2CuO_6$ and $Tl_2Ba_2CuO_6$ represent the $n = 1$ members formed by single perovskite layers according to the formulae $[La_{1-x}M_xCuO_{3-\delta}][La_{1-y}M_yO]$, $[SrCuO_3][(BiO)_2(SrO)]$ and $[BaCuO_3][(TlO_2)(BaO)]$. They differ from one another in the thickness of the rock-salt-type layers. Similarly, $TlCaBa_2Cu_2O_7$, $Bi_2CaSr_2Cu_2O_8$ and $Tl_2CaBa_2Cu_2O_8$, the $n = 2$ members with two oxygen-deficient perovskite-type layers, can be written as $[CaBa(CuO_{2.5}\square_{0.5})_2][(BaO)(TlO)]$, $[CaSr(CuO_{2.5}\square_{0.5})_2][(SrO)(BiO)_2]$ and $[CaBa(CuO_{2.5}\square_{0.5})_2][(BaO)(TlO)_2]$. We can extend this type of formulation to $n = 3$ and higher members. Fig. 12 shows the structures of various cuprate superconductors in this type of formulation.

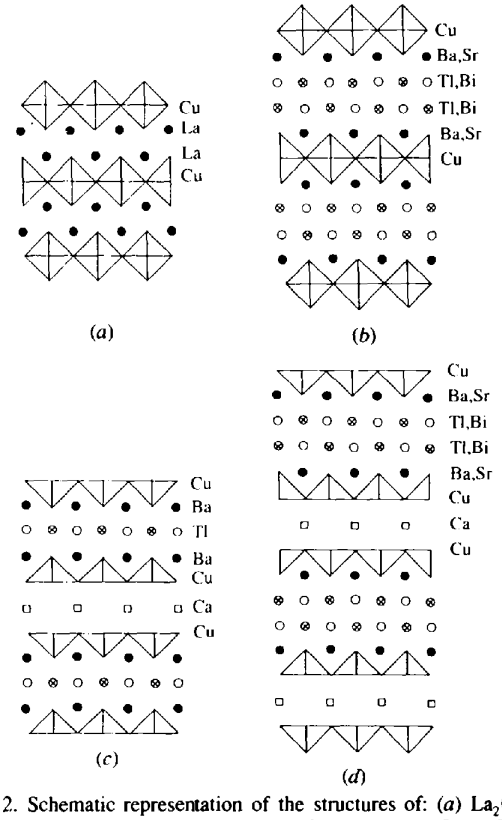

Fig. 12. Schematic representation of the structures of: (*a*) La_2CuO_4; (*b*) $Bi_2Sr_2CuO_6$ and $Tl_2Ba_2CuO_6$; (*c*) $TlCaBa_2Cu_2O_7$; (*d*) $Bi_2CaSr_2Cu_2O_8$ and $Tl_2CaBa_2Cu_2O_8$, showing intergrowth of rock-salt- and perovskite-type layers. O atoms are shown as open circles and Bi and Tl with a cross [from Rao & Raveau (1989)].

Santoro, Beech, Marezio & Cava (1988) have proposed a classification of the copper oxide superconductors in which layers of AO and BO_2 are arranged in such a way as to form perovskite or rock-salt blocks. For example, the sequence of AO and BO_2 layers for $Pb_2Sr_2YCu_3O_8$ is given by $Y(CuO_2)(SrO)(PbO)(Cu)$-$(PbO)(SrO)(CuO_2)(Y)$. In $YBa_2Cu_3O_7$ we have the sequence $(Y)(CuO_2)(BaO)(CuO)(BaO)(CuO_2)(Y)$.

Since all the cuprate superconductors have layered structures, one way of looking at them schematically is to consider the projection of the structure perpendicular to the a or b axes (Verwerft, Van Tendeloo & Amelinckx, 1988). Such a schematic representation of the layers is helpful in visualizing various members of the $Tl_mCa_{n-1}(Ba,Sr)_2Cu_nO_{2n+m+2}$ $(m = 1, 2)$ and the $Bi_2Ca_{n-1}Sr_2Cu_nO_{2n+4}$ series. Other ways of looking at cuprate structures have been described in the literature (Tokura & Arima, 1990; Yoshizaki, 1991).

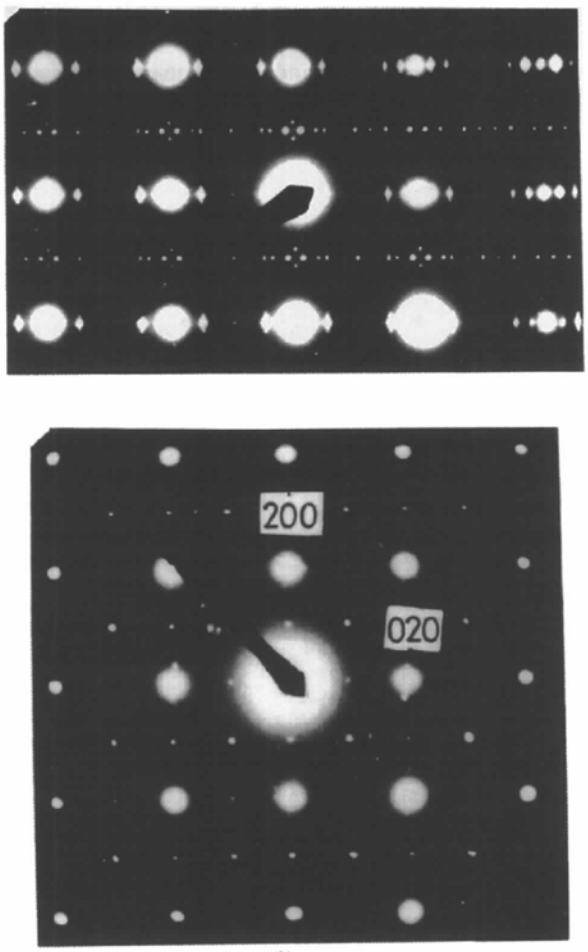

(*b*)

Fig. 13. Electron-diffraction patterns (*a*) of an incommensurately modulated Bi cuprate showing satellites and (*b*) of a modulation-free Bi superconductor, $BiPbSr_2Y_{0.5}Ca_{0.5}Cu_2O_8$ [from Rao, Nagarajan, Vijayaraghavan *et al.* (1990) and Manivannan, Gopalakrishnan & Rao (1991)].

4. Modulation

The incommensurate modulation exhibited by the $Bi_2Ca_{n-1}Sr_2Cu_nO_{2n+4}$ family of cuprates (Rao *et al.*, 1990; Zandbergen, Groen, Mijlhoff, Van Tendeloo & Amelinckx, 1988) has been mentioned earlier. The modulation was explained on the basis of the superspace-group theory of de Wolff, Janssen & Janner (1981). This basically uses one of the 230 crystallographic space groups together with atomic modulation functions which describe the periodic compositional variation and periodic distortions yielding the real structure. In the case of the incommensurately modulated structures, the k-vectors of the Fourier spectrum of atomic modulation functions and the crystal potential of the basic structure are not related by integers and hence are described by four-dimensional space groups. Experimentally, electron-diffraction patterns [Fig. 13(*a*)] show weak reflections (satellites) along with the main reflections which can be described by introducing a fourth index m and an additional basis vector q, $q = \beta b* + \gamma c*$, and hence the diffraction vector H is given as

$$H = ha* + kb* + lc* + mq,$$

where h, k, l and m are integers. Tl cuprates also show features of modulated structures. The modulation is relatively weak compared with those in the Bi cuprates. The occurence of a weak $2q$ modulation in the $n = 1$ and 2 members of Tl cuprate superconductors has been reported (Zandbergen, Groen, Mijlhoff, Van Tendeloo & Amelinckx, 1988); the modulation disappears under electron beam irradiation, suggesting that the modulation is associated with O atoms.

The study of modulation in cuprates has been extensively carried out by a combination of various electron microscopic techniques (Kihlborg, 1990, and references therein; Hewat & Hewat, 1994; Raveau, Michel, Hervieu & Groult, 1991). An HREM image showing modulation is given in Fig. 14. Since good single crystals of Bi superconductors are not easy to grow and the weak modulation in Tl cuprates is difficult

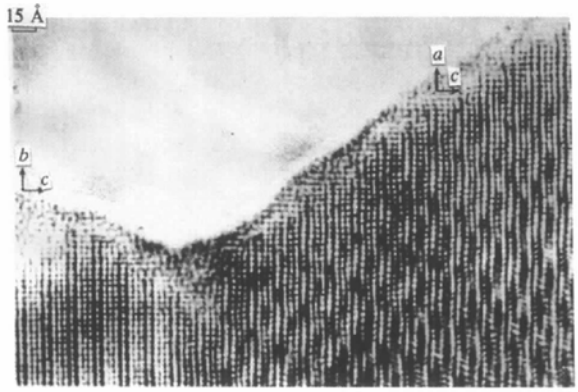

Fig. 14. HREM image of the bismuth cuprate $Bi_2Sr_2CuO_6$, showing modulation [from Raveau, Michel, Hervieu & Groult (1991)].

to study by single-crystal X-ray diffraction, electron microscopy becomes extremely useful. Furthermore, single-crystal X-ray studies are feasible only when the modulation is commensurate. Single-crystal X-ray studies of doped Bi cuprates where Cu is partly substituted by Fe, Mn and Co have been reported (Le Page, McKinnon, Tarascon & Barboux, 1989; Tarascon *et al.*, 1990). In these cases, the modulation is commensurate and thus a full structural refinement was possible. Detailed studies to understand the origin of modulation in these superconductors have led to various models. The various factors considered are (*a*) the role of the extra oxygen, (*b*) displacement of Bi or Tl and (*c*) the lone pair of Bi^{3+}. In Fig. 15 we show a model of the superstructure proposed by Le Page, McKinnon, Tarascon & Barboux (1989). The figure shows how oxygen is moving towards a pair of Bi atoms. This displacement increases along the *x*-axis until oxygen is directly between a pair of Bi atoms. In this way it is possible to fit one extra oxygen for every four or five unit cells, without leading to any interstitial oxygen.

Modulation-free superconductors have been synthesized [*e.g.* $Bi_{2-x}Pb_xSr_{2-y}La_yCuO_6$ and, more recently, $(Bi,Pb)_2(Sr,Ln)_2CuO_6$ (Ln = La,Pr,Nd) and $(Bi,Pb)_2Sr_2Ln_{1-x}Ca_xCu_2O_8$, Ln = Y or rare-earth (Manivannan, Gopalakrishnan & Rao, 1991]. The absence of modulation in lead-doped Bi superconductors [Fig. 13(*b*)] is probably due to the fact that Pb^{2+} reduces the effective charge on the BiO sheets and hence the necessity of extra oxygen (which are possible candidates for causing modulation) within the layers. Several non-superconducting analogues showing modulation are known.

5. Long-period mixed polytypes and intergrowths

In the layered cuprate superconductors, especially the Tl-based ones, there is evidence for the formation of mixed-layer polytypes involving complex layer sequences. Such long stacking sequences have been observed (Verwerft, Van Tendeloo & Amelinckx, 1988) by electron microscopy and are normally seen at low magnifcation and in the thicker parts of the specimen. The 00*l* sequence of spots in the electron-diffraction patterns show streaking (made up of very closely spaced diffraction spots). High-resolution images show variability in the thickness of the perovskite blocks and also in the number of Tl—O layers. Mixed-layer polytypism is presumably a consequence of spiral growth, as found in Bi-based superconductors (Hayashi, Ohno, Iuoue & Komatsu, 1988).

Intergrowths of different *n* members (differing in the number of CuO_2 sheets), as in $Bi_2(Ca,Sr)_{n+1}Cu_nO_{2n+4}$, are commonly observed in the HREM images of cuprate superconductors. These are examples of non-recurrent intergrowth. In the $Tl_2Ca_{n-1}Ba_2Cu_nO_{2n+4}$ series, non-recurrent intergrowth of $n = 2$ and 3 members has been seen. Intergrowth of the higher members (*e.g.* $n = 5$) in the $n = 2$ phase has been occasionally seen in electron-diffraction patterns (Fig. 16) and HREM images (Ganguli *et al.*, 1988). Intergrowths involving $n = 5$ and 7 members have been observed in HREM images of the 2324 Tl superconductors by Raveau, Michel, Hervieu & Groult (1991). Intergrowth defects involving a rock-salt layer (*e.g.* intergrowth of Tl-1212 and Tl-2122 members) have also been observed (Raveau Michel, Hervieu & Groult, 1991). It appears that the triple rock-salt layer $[(BaO)(TlO)_2]$ intergrows with double [(BaO)(TlO)] layers. Intergrowths have been observed in fluorite-layered cuprates such as $TlBa_2NdCu_2O_7$, where the double-fluorite layer intergrows with the rock-salt layer. The effect of intergrowths on the superconducting properties of cuprates is not fully understood, although it appears to be marginal.

6. Local disorder and oxygen defects

Most of the cuprate superconductors contain defects. These defects may be due to substitutions at metal sites, vacancies either in the metal or in the oxygen sites, interstitial oxygen or excess oxygen present due to the modulation of atomic displacements. Other than these defects, many of the cuprate superconductors have stacking faults, dislocations and intergrowths. The origin

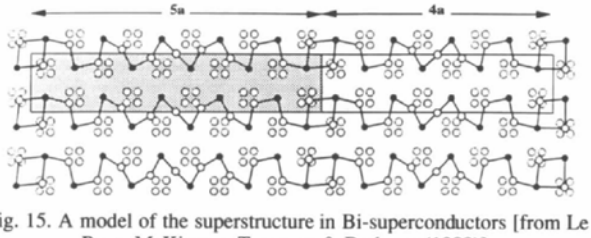

Fig. 15. A model of the superstructure in Bi-superconductors [from Le Page, McKinnon, Tarascon & Barboux (1989)].

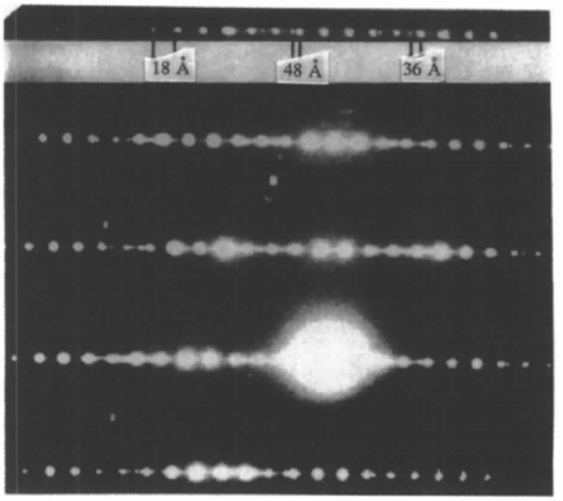

Fig. 16. Electron-diffraction pattern of a Tl–Ca–Ba–Cu–O sample, showing discrete diffraction spots corresponding to 36 ($n = 3$) and 48 Å ($n = 5$) [from Ganguli *et al.* (1988)].

and nature of defects is of relevance to understand the mechanism of superconductivity, especially in those cases where defects (*e.g.* Tl deficiency in single Tl—O layer cuprates) are dope charge carriers. Oxygen excess in many Tl cuprates renders them non-superconducting. Extended defects such as stacking faults, dislocations and intergrowths are readily investigated by electron microscopy (Raveau, Michel, Heriveu & Groult, 1991). In order to understand defects caused by local structural disorder, pulsed neutron data has been analysed to yield atomic pair distribution functions. Such data have indicated significant deviations in the positions of the atoms obtained earlier by X-ray crystallography. In $Tl_2CaBa_2Cu_2O_8$, short-range ordering resulting from displacements of Tl and O in the Tl—O plane has been established (Fig. 17). The ordering results in Tl—O chains or Tl_2O_2 clusters. Such local ordering appears to create space large enough for some extra oxygen. Such interstitial oxygens have actually been found in $Bi_2Sr_2CaCu_2O_8$ and $Tl_2Ba_2CuO_{6-\delta}$. The appearance of weak modulation in Tl superconductors is a result of such local order in the Tl—O plane.

An interesting example of oxygen interstitials is $La_2CuO_{4+\delta}$ (Dabrowski *et al.*, 1989; Jorgensen, 1991), where the excess oxygen moves towards the interstitial site (Fig. 18), thereby creating charge carriers and superconductivity. The superconducting compound is formed by a phase separation process. On cooling below room temperature, interstitial oxygens form a phase with $\delta = 0.08$, which is superconducting, while the phase with $\delta = 0.0$ is antiferromagnetic and non-superconducting. Doping here is identical to that in $La_{1.85}Sr_{0.15}CuO_4$ and both have comparable T_c's of around 35 K. The $\delta = 0.08$ and 0.00 phases of $La_2CuO_{4+\delta}$ belong to *Fmmm* and *Bmab* space groups, respectively. In non-superconducting $La_2NiO_{4+\delta}$ also a similar oxygen interstitial defect has been found (Jorgensen, Dabrowski, Pei, Richards & Hinks, 1989). It should be noted that the interstitial position occupied by the excess oxygen was not clear from neutron diffraction studies on $La_2CuO_{4+\delta}$, but studies on $La_2NiO_{4+\delta}$ (which is similar to $La_2CuO_{4+\delta}$) revealed the interstitial position unambiguously. Unusual excess oxygen-containing nickelates have been described recently (Demourges *et al.*, 1993).

7. Correlaton of T_c with structural parameters

A common structural feature in all the superconducting cuprates is the presence of two-dimensional CuO_2 sheets. These CuO_2 sheets contain the delocalized holes which are responsible for superconductivity. Modifying the CuO_2 sheets by structural distortion or ion substitution does not favour superconductivity. In fluorite-type superconductors with two CuO_2 sheets, the fluorite-layers (Ln_2O_2), which are between CuO_2 sheets, dramatically lower the T_c, thereby indicating that distancing the CuO_2 sheets is unfavourable to superconductivity (see, for example, Arima *et al.*, 1990; Vijayaraghavan *et al.*, 1993). On the contrary, I_2 intercalated within the BiO layers (Xiang *et al.*, 1990)

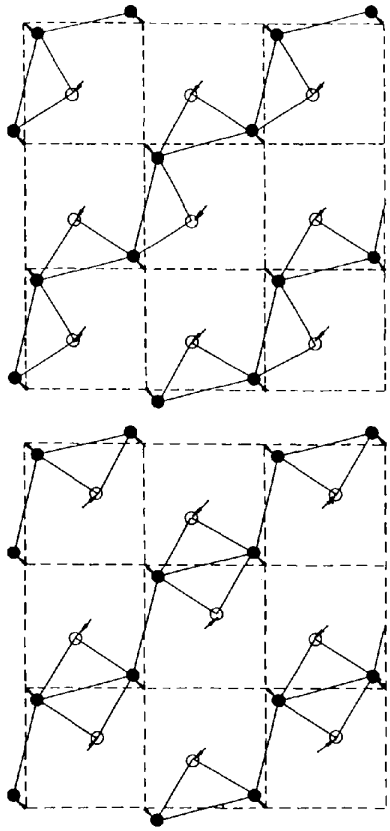

Fig. 17. Short-range ordering in the Tl—O layer observed in $Tl_2CaBa_2Cu_2O_8$ [from Dmowski *et al.* (1988)].

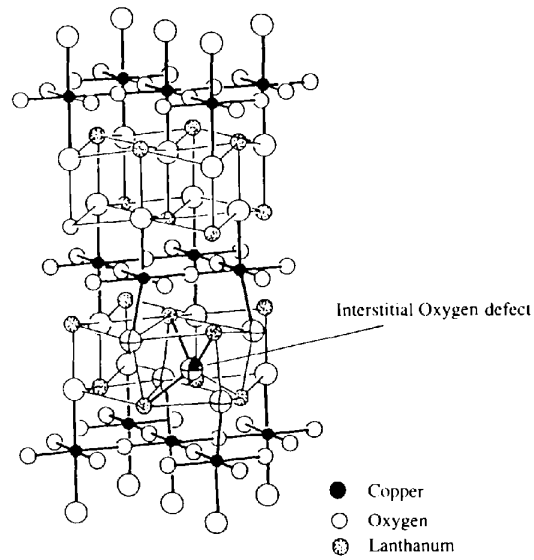

Fig. 18. The structure of $La_2CuO_{4+\delta}$ showing the interstitial oxygen [from Dabrowski *et al.* (1989)].

in $Bi_2CaSr_2Cu_2O_8$ does not reduce T_c appreciably. The value of T_c increases with the number of CuO_2 sheets n in each family of superconducting cuprates until it reaches a maximum at $n = 3$ and then decreases. This can be seen in Fig. 19 where we show T_c *versus* n plots for five families of superconducting cuprates, including the recently discovered $HgCa_{n-1}Ba_2Cu_nO_{2n+2+\delta}$. We see that only the $TlCa_{n-1}Ba_2Cu_nO_{2n+3}$ cuprates show a maximum in T_c for the $n = 4$ member. The Hg-1234 cuprate is reported to have a lower T_c than the 1223 member (Capponi *et al.*, 1993, and references therein).

7.1. *Relation between T_c and the in-plane* Cu—O *distance*

In an ideal perovskite, the B-cation occupies an octahedral site and the BO_6 octahedra are corner-shared in three directions. In the superconducting cuprates we have a variety of possible Cu—O polyhedra. Thus, we have CuO_6 units in $La_{2-x}Sr_xCuO_4$, $Tl_2Ba_2CuO_6$ and $Bi_2Sr_2CuO_6$, CuO_5 units in the $n = 2$ member of Tl, Bi and Hg cuprates, CuO_4 and CuO_5 units in $LaBa_2Cu_3O_{7-\delta}$, as well as in the $n = 3$ members of Tl, Bi and Hg cuprates, and in the T^* structure of $Nd_{2-x-y}Ce_xSr_yCuO_y$. Only CuO_4 units are present in $Nd_{2-x}Ce_xCuO_4$ and $Sr_{2-x}Nd_xCuO_y$. All the above cuprates are normally considered to have CuO_2 sheets, where each Cu has either two apical oxygens (CuO_6), one apical oxygen (CuO_5) or no apical oxygen (CuO_4). The CuO_2 sheet in the cuprates is the most important structural component necessary for superconductivity, with the charge carriers (holes or electrons) being delocalized over the sheets. The a-parameter is roughly twice the in-plane Cu—O bond length in the cuprates. The in-plane Cu—O bonds are antibonding in nature (Whangbo & Torardi, 1991) and hole-doping therefore generally reduces the length of the in-plane bonds. In many instances, substitution of larger atoms (steric factor) does not overcome this electronic factor and the a-parameter decreases, although the c-parameter increases.

From this discussion, we can surmise how the hole concentration n_h in cuprate superconductors would be reflected in the in-plane Cu—O bond distances. Where accurate n_h values are not known, a plot of T_c *versus* the in-plane Cu—O distance provides a means of studying the T_c *versus* n_h relation. This is especially so in the case of Tl-based superconductors, where good n_h values are difficult to obtain by chemical analysis. We show in Fig. 20 r(Cu—O) *versus* T_c correlations in some Tl cuprates with T_c maxima at optimal Cu—O bond lengths (reflecting optimal n_h values). It should be recalled that T_c attains a maximum value at an optimal n_n value in

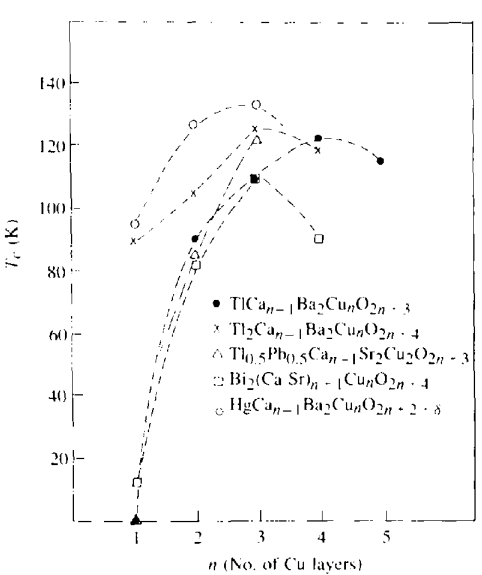

Fig. 19. Variation of T_c with the number of CuO_2 sheets in five different families of cuprates.

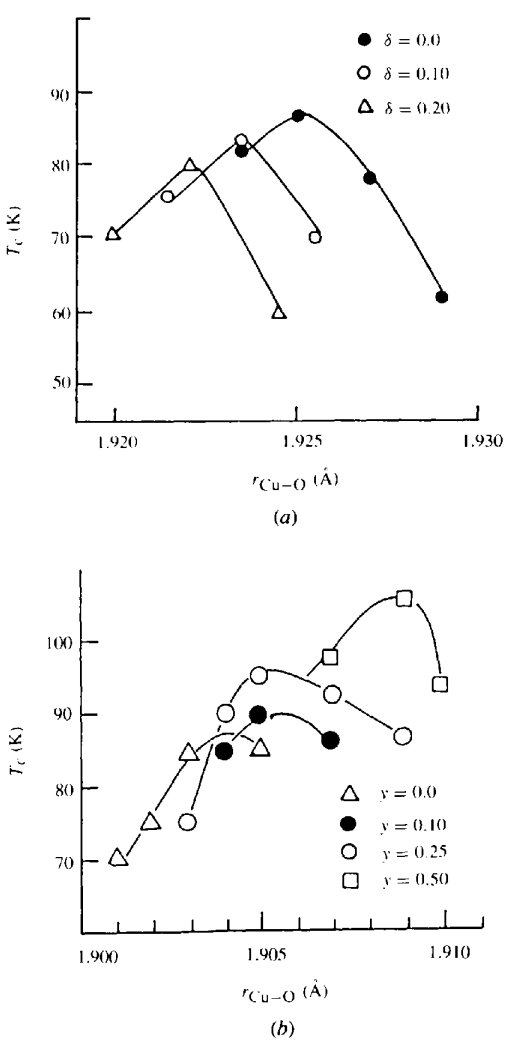

Fig. 20. Variation of T_c with the Cu—O distance in (*a*) $Tl_{1-\delta}Y_{1-x}Ca_xBa_2Cu_2O_7$ and (*b*) $Tl_{1-y}Pb_yY_{1-x}Ca_xSr_2Cu_2O_7$ [adapted from Rao (1994)].

cuprates (Rao, Gopalakrishnan, Santra & Manivannan, 1991). Such correlations were proposed by Whangbo, Kang & Torardi (1989) for $Tl_mCa_{n-1}Ba_2Cu_nO_{2n+m+\delta}$ ($m = 1, 2$; $n = 1, 2, 3$), $(Tl_{0.5}Pb_{0.5})(Ca_{n-1}Sr_2Cu_nO_{2n+3})$ and $Bi_2Ca_{n-1}Sr_2Cu_nO_{2n+4}$ along with $La_{2-x}Sr_xCuO_4$-related structures. Three distinct classes of T_c *versus* r(Cu—O) correlations were observed, depending on the cation located above and below the CuO_2 sheets, at the nine coordinated sites. Each class seems to have an optimum value of the Cu—O distance for which T_c is maximum. The Ba class seems to exhibit the highest T_c's.

In Fig. 21, we have plotted reduced T_c values (T_c/T_c max) with the in-plane r(Cu—O) distance for several families of cuprate superconductors. The plot shows an interesting behaviour with all the highest T_c cuprates falling within the Cu—O distance range ~1.89–1.94 Å. Members with low r(Cu—O) < 1.88 Å tend to be metallic, while those with r(Cu—O) > 1.94 Å tend to be insulating. The plot still shows different insulator boundaries at large r(Cu—O) for the different cation families.

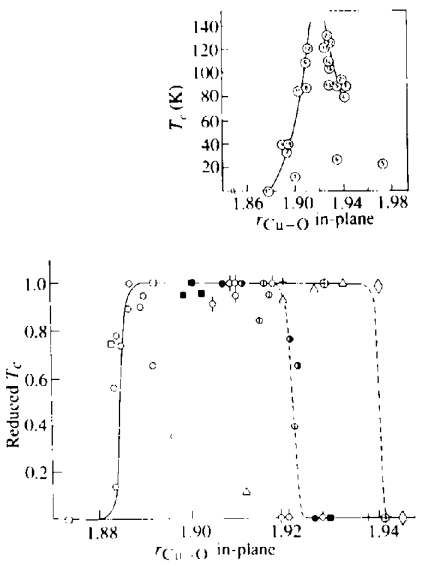

Fig. 21. Plot of reduced T_c with in-plane r(Cu—O) distance: $La_{2-x}Sr_xCuO_4$ (open circles), $YBa_2Cu_3O_{7-\delta}$ (circles with cross), $Bi_2(Ca,Y,Sr)_3Cu_2O_8$ (half-shaded circles), $Bi_2Ca_{1-x}Y_xSr_2Cu_2O_8$ (circles with a dividing line), modulation-free Bi cuprates (filled squares), $TlSr_{2-x}La_xCuO_5$ (open squares), $Tl_2Ba_{2-x}Sr_xCuO_6$ (open triangles), $TlCa_{1-x}Y_xBa_2Cu_2O_7$ (cross), $TlCa_{1-x}Ln_xSr_2Cu_2O_7$ (circles with one line on top), $Tl_{0.5}Pb_{0.5}Ca_{1-x}Y_xSr_2Cu_2O_7$ (circles with one line on top and one at the bottom), $Pb_2Sr_2Y_{1-x}Ca_xCu_3O_{8+\delta}$ (filled circles) and $HgBa_2CuO_{4+\delta}$ (open diamonds). Inset shows the variation of T_c with in-plane Cu—O distance considering only the cuprates showing the maximum T_c in each family. (1) $La_{1.85}Sr_{0.15}CuO_4$; (2) $La_{1.85}Ba_{0.15}CuO_4$; (3) $YBa_2Cu_3O_{6.91}$; (4) $YBa_2Cu_4O_8$; (5) $Nd_{1.85}Ce_{0.15}CuO_4$; (6) $Nd_{1.4}Ce_{0.2}Sr_{0.4}CuO_4$; (7) $Bi_2Sr_2CuO_6$; (8) $Bi_2CaSr_2Cu_2O_8$; (9) $Bi_2Ca_2Sr_2Cu_3O_{10}$; (10) $Tl_{0.5}Pb_{0.5}Sr_2CuO_5$; (11) $Tl_{0.5}Pb_{0.5}CaSr_2Cu_2O_7$; (12) $Tl_{0.5}Pb_{0.5}Ca_2Sr_2Cu_3O_9$; (13) $TlCaBa_2Cu_2O_7$; (14) $TlCa_2Ba_2Cu_3O_9$; (15) $Tl_2Ba_2CuO_6$; (16) $Tl_2CaBa_2Cu_2O_8$; (17) $Tl_2Ca_2Ba_2Cu_3O_{10}$; (18) $Tl_2Ca_3Ba_2Cu_4O_{12}$; (19) $TlSrLaCuO_5$; (20) $TlCa_{0.5}La_{0.5}Sr_2Cu_2O_7$; (21) $HgBa_2CuO_{4.065}$; (22) $HgCaBa_2Cu_2O_{6.22}$; (23) $HgCa_2Ba_2Cu_3O_{8.41}$.

Instead of considering the entire range of T_c values in each family of cuprates (*e.g.* in $Bi_2Ca_{1-x}Y_xSr_2Cu_2O_8$), if we consider only the maximum T_c in each family [*e.g.* $YBa_2Cu_3O_{6.91}$ with a T_c of 90 K in the $YBa_2Cu_3O_{7-\delta}$ family, $La_{1.85}Sr_{0.15}CuO_4$ (40 K) in $La_{2-x}Sr_xCuO_4$ and $TlCaBr_2Cu_2O_7$ not $TlCa_{1-x}Y_xBa_2Cu_2O_7$], we obtain a universal curve shown in the inset of Fig. 21, which peaks around ~1.920 Å. In this correlation, maximum T_c compositions (23 in total) of the different families of cuprates and the corresponding in-plane Cu—O bond distances have been considered. $Bi_2Sr_2CuO_6$ with $T_c = 12$ K does not fall on the curve. This may be rationalized by the fact that $Bi_2Sr_2CuO_6$ is not the cuprate with the maximum T_c in the $n = 1$ family of bismuth cuprates. With optimum doping as in $Bi_2Sr_{2-x}La_xCuO_{6+\delta}$ (Groen, De Leeuw & Geelan, 1990), a higher $T_c \sim 30$ K can be obtained, which falls on the curve. We have not tried to force the T^* and T' data points on this curve. The plot in the inset of Fig. 21 indicates that the maximum possible value of T_c in cuprates will be found at Cu—O distances of 1.92 Å.

7.2. *Relation between T_c and the apical* Cu—O *distance*

We discussed earlier how the planar CuO_2 sheets are the seat of superconductivity in cuprates. Although the Cu $d_{x^2-y^2}$ bands are not expected to overlap with the s and p orbitals of the apical oxygen, they do indirectly affect superconductivity in the cuprates. It has been shown earlier that the Cu—O apical bond lengths may be related to T_c *via* bond-valence sums (Tallon & Williams, 1990). The presence of apical oxygens is necessary for hole-doping in the CuO_2 sheets. Cuprates having CuO_2 sheets (CuO_4 planar units) with no apical oxygens have not been doped with holes until now (note that T' $Nd_{2-x}Ce_xCuO_4$ and $Sr_{1-x}Nd_xCuO_y$ are electron-doped). Also, cuprate superconductors with apical oxygens (*e.g.* Y-124, the T^* phase of $Nd_{2-x-y}Ce_xSr_yCuO_4$, Hg-1223) show a large pressure enhancement of T_c (Nunez-Regueiro, Tholence, Antipov, Capponi & Marezio, 1993; Kaldis *et al.*, 1989), whereas in the superconducting cuprates without apical oxygens (T' phases) the pressure coefficient of T_c is small.

We have tried to examine whether any interesting correlation exists between the apical Cu—O distance and T_c in the superconducting cuprate families, considering only those compositions corresponding to the maximum T_c value in each family. We do not find a universal curve or region to describe the correlation with T_c. However, we find that within a series of cuprates with a varying number of CuO_2 sheets, T_c increases with a decrease in the apical Cu—O distance.

A direct relation between T_c and the apical Cu—O bond length has been found by Cava *et al.* (1990) in $YBa_2Cu_3O_{7-\delta}$. In this system, the variation of T_c with δ

mirrors the variation of the apical distance. A definitive correlation between the Cu—O apical distance and T_c is found in $YBa_2Cu_4O_8$. Nelmes, Loveday, Kaldis & Karpinski (1992) have shown that on applying pressure, the T_c of $YBa_2Cu_4O_8$ increases from 80 to 90 K, while the apical distance shortens. In a related study on the influence of apical oxygen on the superconducting transition temperatures (Ohta, Tohyama & Maekawa, 1991), the importance of the energy level of the apical oxygen has been pointed out.

7.3. *Relation between T_c and Madelung potentials*

Torrance & Metzger (1989) were probably among the first to point out the importance of the Madelung site potential ΔV_M in the hole conductivity of the cuprate superconductors. Here ΔV_M is the difference in Madelung site potential for a hole on a Cu site and that on an oxygen site. Following their analysis, two classes of compounds were demarcated, those with high ΔV_M ($\geq$ 47 eV) being metallic and superconducting and those with lower ΔV_M being semiconducting (with localized holes). Ohta, Tohyama & Maekawa (1991), using the ionic model, have calculated the Madelung site potential (which is a measure of the one-body energy level of each orbital) and obtained the position of the energy levels for the $3d_{x^2-y^2}$ and $3d_{z^2}$ orbitals of Cu, and the $2p$ orbitals of the apical and the in-plane O atoms. These workers propose that the position of the energy level of the apical O atoms is of primary importance for the electronic states of the CuO_2 plane and governs the optimum T_c's of all the families of hole superconductors. A scaling parameter for T_c, ΔV_A has been proposed, where ΔV_A is the difference in the Madelung site potentials for a hole between the apex and the in-plane O atoms and is a measure of the position of the energy level of the P_z-orbital on apical oxygens. The maximum T_c's (optimum hole doping) of hole-doped cuprates fall on a curve (with some width), cuprates with large ΔV_A exhibiting high T_c's. It appears that the energy level of the apical O atom plays a significant role in the electronic states of the doped holes, thereby affecting T_c. The origin of such a correlation is ascribed to the stability of local singlet states made up of two holes in the Cu $3d_{x^2-y^2}$ and O $2p_\sigma$ orbitals in the CuO_2 plane. The local singlet is well defined and stable when the energy level of the apex O atom is sufficiently high. A comparison of the correlations of T_c with ΔV_A and ΔV_M suggests that ΔV_A scales better with T_c.

7.4. *Bond valence sums and T_c*

The bond valence sum for an atom i over each of its nearest neighbour atoms j is given by (Brown & Altermatt, 1985)

$$V_i = \sum_j \exp(R_O - R_{ij})/0.37,$$

where R_{ij} is the distance between atoms i and j. The sum is a measure of the total charge on an atom in a structure and changes in the sum with oxygen doping; cation substitution or applied pressure is an indication of charge transfer within the structure. Defining $V_- = 2 + V_{Cu2} - V_{O2} - V_{O3}$, where V_- is the total excess charge in the planes [O2 and O3 are the oxygen in the plane], $V_+ = 6 - V_{Cu2} - V_{O2} - V_{O3}$ defines the preferential distribution of this charge on the oxygen sites (Tallon & Williams, 1990). Interestingly, the T_c *versus* V_- plot for $YBa_2Cu_3O_{7-\delta}$ mirrors the T_c *versus* δ plot. The V_+ parameter against T_c is nearly a straight line with a slope of unity.

8. 123→124 transformation in $YBa_2Cu_3O_{6.7}$ (60 K phase)

The 60 K T_c plateau region of $YBa_2Cu_3O_{7-\delta}$ ($0.3 \leq \delta \leq 0.4$) has been the subject of considerable investigation. Compositions in this range show diffuse scattering or superlattice spots in the electron diffraction patterns, but such diffraction spots could arise from mixtures or, more likely, intergrowths of differently ordered oxygen-deficient phases (Rao, Nagarajan, Ganguli *et al.*, 1990). Accordingly, we observe weak Cu^{2+} EPR signals in these compositions. Compositions in the δ range 0.3–0.4 are metastable arising from a rather disordered oxygen vacancy arrangement with a tendency to transform into more stable phases. Heating orthorhombic $YBa_2Cu_3O_{6.7}$ ($T_c \sim 60$ K) for 50–100 h at 470 K in air (Fig. 22) leads to a structure with $c \sim n \times 13.5$ Å, suggesting the formation of a 124 type phase (note that the c-parameter of $YBa_2Cu_4O_8$ is 27 Å). The X-ray diffraction pattern of the annealed sample has very few lines compared with that of $YBa_2Cu_4O_8$ (Nagarajan & Rao, 1993). Evidence of disorder in the 470 K annealed samples is also provided by the electron-diffraction patterns, where marked streaking is noticed along the c-

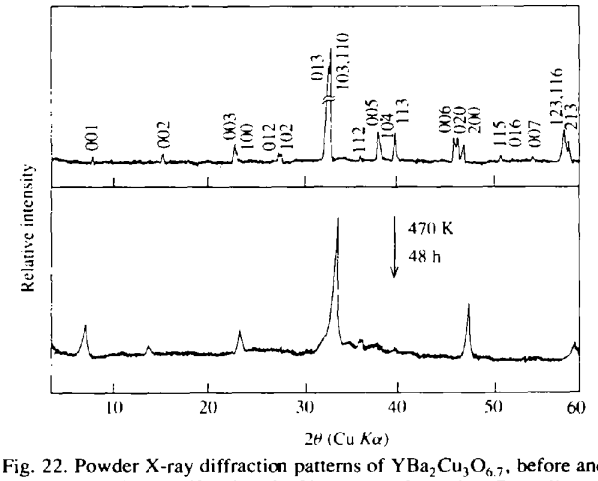

Fig. 22. Powder X-ray diffraction patterns of $YBa_2Cu_3O_{6.7}$, before and after annealing at 470 K for 48 h [from Rao, Nagarajan, Ganguli *et al.* (1990)].

axis. This is probably due to the absence of registry along the *c*-axis caused by the extensive oxygen disorder in the *ab* plane. Accordingly, twins are not observed in the bright field image of the product after thermal treatment, while the starting $YBa_2Cu_3O_{6.7}$ shows extensive twinning.

HREM lattice images (Fig. 23) show 13.5 Å fringes in the annealed sample along the *c*-axis, which also suggests the existence of 124 or 247 types of phases. It is proposed that this phase is possibly a highly disordered 124-type phase, which is a precursor to the decomposition or disproportionation that occurs on heating $YBa_2Cu_3O_{6.7}$ for longer periods of about 200 h or more. Metastable forms of $YBa_2Cu_4O_8$ involving a body-centred lattice, instead of the *A* centring (*Ammm*) present in bulk $YBa_2Cu_4O_8$, are considered to be the likely products. An *I*-centred $YBa_2Cu_4O_8$ can be generated by shear operation of half the unit cell of $YBa_2Cu_3O_7$ by $a/2$ (Fig. 24). The computed X-ray diffraction pattern based on such an *I*-centred cell (*Immm*) seems to be much closer to the observed X-ray diffraction pattern of the annealed 123 sample (Nagarajan & Rao, 1993).

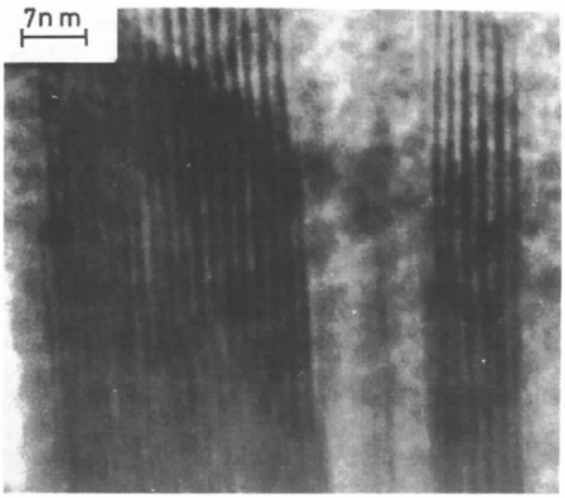

Fig. 23. HREM image showing 13.5 Å fringes in $YBa_2Cu_3O_{6.7}$ annealed in air at 470 K for 48 h [from Rao, Nagarajan, Ganguli *et al.* (1990)].

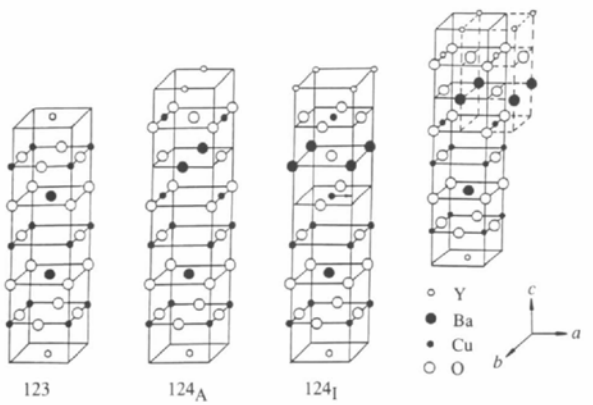

Fig. 24. Schematic structures of the *A*-centred and the hypothetical *I*-centred unit cells of $YBa_2Cu_4O_8$, along with a possible shear operation mechanism for the transformation from the *A* to the *I*-centred cell [from Nagarajan & Rao (1993)].

9. Oxyanion derivatives of cuprates

A remarkable discovery in the last three years is the possibility of incorporating oxyanions such as carbonate and nitrate as integral parts of cuprate structures. Carbonate derivatives of cuprates such as $YBa_2Cu_3O_7$, as well as the infinite-layered $Sr_2CuO_2CO_3$ prepared early in this effort, were not superconducting. However, many superconducting oxyanion derivatives of cuprates have since been prepared, making them more interesting. What is surprising is that some of these cuprates cannot be prepared as stable phases in the absence of the oxyanions. An interesting 123 cuprate is that obtained by incorporating both CO_3^{2-} and NO_3^-, with the general formula $YBa_{2-x}Sr_xCu_{2.5}(CO_3)_{0.5-x}(NO_3)_xO_y$ (Fig. 25); without NO_3^- the cuprate is not superconducting (Maignan, Hervieu, Michel & Raveau, 1993; Rao *et al.*, 1993). $YSr_2Cu_3O_7$ cannot be prepared in pure form, but can be stabilized by incorporation of PO_4^{3-} (Fig. 26)

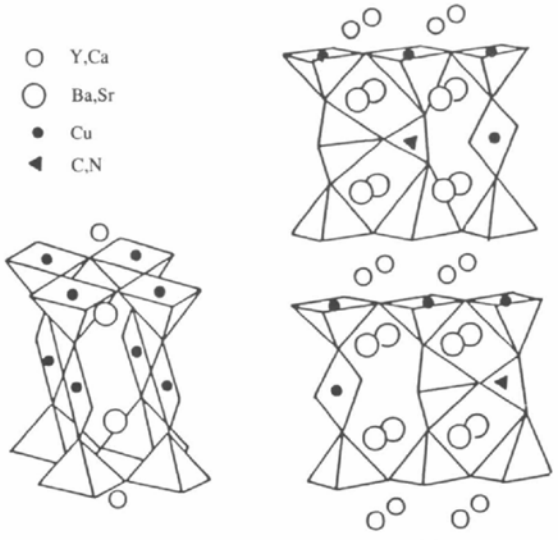

Fig. 25. Schematic structures of (*a*) $YBaSrCu_3O_{7-\delta}$ and (*b*) $Y_2Ba_2Sr_2Cu_5(CO_3)_{1-x}(NO_3)_xO_y$ [from Rao *et al.* (1993)].

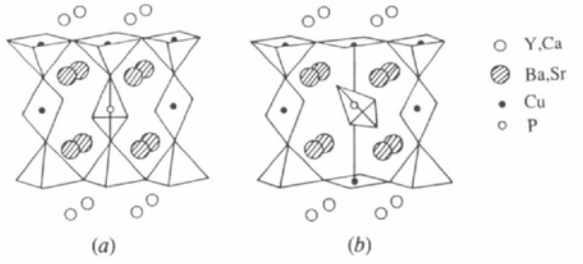

Fig. 26. Schematic structures of the phosphate derivative of the Y–Sr–Cu–O (123) system [from Nagarajan, Ayyappan & Rao (1994)].

and rendered superconducting by partial replacement of Y by Ca (Nagarajan, Ayyappan & Rao, 1994). In the 123 cuprates, the oxyanion generally replaces the CuO_4 group in the Cu—O chains (Fig. 25). In Fig. 26 we show the schematic diagram of a superconducting phosphate derivative of a 123 cuprate to show how the PO_4^{3-} tetrahedra would have to be arranged in order to favour the creation of holes. It is well known that the maximum T_c in the $Bi_2Sr_2CuO_6$ system is 22 K, but by the incorporation of CO_3^{2-} a T_c of 30 K has been obtained (Pelloquin *et al.*, 1993). This is remarkable indeed. It is not exactly clear how the oxyanions are involved in the creation, or otherwise, of charge carriers. Structural aspects of the oxyanion derivatives are yet to be fully established.

The authors thank the Science Office of the European Union, Department of Science and Technology, Government of India and the US National Science Foundation for support of the work.

References

AL-MAMOURI, M., EDWARDS, P. P., GREAVES, C. & SLASKI, M. (1994). *Nature*, **369**, 382–384.

ARIMA, T., TOKURA, Y., TAKAGI, H., UCHIDA, S., BEYERS, R. & TORRANCE, J. B. (1990). *Physica C*, **168**, 79–84.

AZUMA, M., HIROI, Z., TAKANO, M., BANDO, Y. & TAKEDA, Y. (1992). *Nature*, **356**, 775–776.

BEDNORZ, J. G. & MÜLLER, A. (1986). *Z. Phys. Chem. Abt. B*, **64**, 189–193.

BORDET, P., CHAILLOUT, C., CHENAVAS, J., HODEAU, J. L., MAREZIO, M., KARPINSKI, J. & KALDIS, E. (1988). *Nature*, **334**, 596–598.

BROWN, I. D. & ALTERMATT, D. (1985). *Acta Cryst.* B**41**, 244–247.

CAPPONI, J. J., MAREZIO, M., LOUREIRO, S., CHAILLOUT, C., BORDET, P., CHMAISSEM, O., HUANG, Q., SANTORO, A., PUTILIN, S., ANTIPOV, E. V., NUNEZ-REGUEIRO, M. & THOLENCE, J. L. (1993). *Superconducting Materials*, edited by J. ETOURNEAU, pp. 27–32. France: IITT International.

CAVA, R. J., HEWAT, A. W., HEWAT, E. A., BATLOGG, B., MAREZIO, M., RABE, K. M., KRAJEWSKI, J. J., PECK, W. F. & RUPP, L W. (1990). *Physica C*, **165**, 419–433.

CAVA, R. J., MAREZIO, M., KRAJEWSKI, J. J., PECK, W. F., SANTORO, A. & BEECH, F. (1989). *Physica C*, **157**, 272–278.

CAVA, R. J., SANTORO, A., JOHNSON, D. W. & RHODES, W. W. (1987). *Phys. Rev. B*, **35**, 6716–6720.

DABROWSKI, B., JORGENSEN, J. D., HINKS, D. G., PEI, S., RICHARDS, D. R., VANFLEET, H. B. & DECKER, D. L. (1989). *Physica C*, **162–164**, 99–100.

DEMOURGES, A., WATTIAUX, A., GRENIER, J. C., POUCHARD, M., SOUBEYROUX, J. L., DANCE, I. M. & HAGENMULLER, P. (1993). *J. Solid State Chem.* **105**, 458–468.

DMOWSKI, W., TOBY, B. H., EGAMI, T., SUBRAMANIAN, M. A., GOPALAKRISHNAN, J. & SLEIGHT, A. W. (1988). *Phys. Rev. Lett.* **61**, 2608–2611.

ER, G., MIYAMOTO, Y., KANAMARU, F. & KIKKAWA, S. (1991). *Physica C*, **181**, 206–208.

GANGULI, A. K., MANIVANNAN, V., SOOD, A. K. & RAO, C. N. R. (1989). *Appl. Phys. Lett.* **55**, 2664–2666.

GANGULI, A. K., NANJUNDASWAMY, K. S. & RAO, C. N. R. (1988). *Physica C*, **156**, 788–790.

GANGULI, A. K., NANJUNDASWAMY, K. S., SUBBANNA, G. N., RAJUMON, M. K., SARMA, D. D. & RAO, C. N. R. (1988). *Mod Phys. Lett. B*, **2**, 1169–1176.

GANGULI, A. K., RAO, C. N. R., SEQUEIRA, A. & RAJAGOPAL, H. (1989). *Z. Phys. Chem. Abt. B*, **74**, 215–219.

GOODENOUGH, J. B. & MANTHIRAM, A. (1991). *Chemistry of High Temperature Superconductors*, edited by C. N. R. RAO, pp. 1–56. Singapore: World Scientific.

GROEN, W. A., DE LEEUW, D. M. & GEELAN, G. P. J. (1990). *Physica C*, **165**, 305–307.

HAYASHI, S., OHNO, T., IUOUE, T. & KOMATSU, H. (1988). *J. Cryst. Growth*, **91**, 331–333.

HEWAT, A. W. & HEWAT, E. A. (1994). *Thallium-based High-Temperature Superconductors*, edited by A. M. HERMANN & J. V. YAKHMI, pp. 89–117. New York: Marcel Dekker.

HEWAT, A. W., FISCHER, P., KALDIS, E., HEWAT, E. A., JILEK, E., KARPINSKI, J. & RUSIECKI, S. (1990). *J. Less Common Met.* **164–165**, 39–49.

JAMES, A. C. W. P., ZAHURAK, S. M. & MURPHY, D. W. (1989). *Nature*, **338**, 240–241.

JORGENSEN, J. D. (1991). *Phys. Today*, **44**, 34–40.

JORGENSEN, J. D., DABROWSKI, B., PEI, S., RICHARDS, D. R. & HINKS, D. G. (1989). *Phys. Rev. B*, **40**, 2187–2199.

KALDIS, E., FISCHER, P., HEWAT, A. W., HEWAT, E. A., KARPINSKI, J. & RUSIECKI, S. (1989). *Physica C*, **159**, 668–680.

KIHLBORG, L. (1990). *Prog. Solid State Chem.* **20**, 101–133.

KOPNIN, E. M., KHARLANOV, A. K., BRYNTSE, I. & ANTIPOV, E. V. (1994). *Physica C*, **219**, 47–56.

LE PAGE, Y., MCKINNON, W. R., TARASCON, J. M. & BARBOUX, P. (1989). *Phys. Rev. B*, **40**, 6810–6816.

MAIGNAN, A., HERVIEU, M., MICHEL, C. & RAVEAU, B. (1993). *Physica C*, **208**, 116–120.

MANIVANNAN, V., GOPALAKRISHNAN, J. & RAO, C. N. R. (1991). *Phys. Rev. B*, **43**, 8686–8689.

MANIVANNAN, V., RANGAVITTAL, N., GOPALAKRISHNAN, J. & RAO, C. N. R. (1993). *Physica C*, **208**, 253–258.

MARKERT, J. T., EARLY, E. A., BJORNHOLM, T., GHAMATY, S., LEE, B. W., NEUMEIER, J. J., PRICE, R. D., SEAMAN, C. L. & MAPLE, M. B. (1989). *Physica C*, **158**, 178–182.

NAGARAJAN, R. & RAO, C. N. R. (1993). *J. Solid State Chem.* **103**, 533–538.

NAGARAJAN, R., AYYAPPAN, S. & RAO, C. N. R. (1994). *Physica C*, **220**, 373–376.

NELMES, R. J., LOVEDAY, J. S., KALDIS, E. & KARPINSKI, J. (1992). *Physica C*, **172**, 311–324.

NUNEZ-REGUEIRO, M., THOLENCE, J. L., ANTIPOV, E. V., CAPPONI, J. J. & MAREZIO, M. (1993). *Science*, **262**, 97–99.

OHTA, Y., TOHYAMA, T. & MAEKAWA, S. (1991). *Phys. Rev. B*, **43**, 2968–2982.

PELLOQUIN, D., CALDES, M., MAIGNAN, A., MICHEL, C., HERVIEU, M. & RAVEAU, B. (1993). *Physica C*, **208**, 121–129.

PLAKHTY, V., STRATILATOV, A., CHERNENKOV, YU., FEDOROV, V., SINHA, S. K., LOONG, C. K., GAULIN, B., VLASOV, M. & MOSHKIN, S. (1992). *Solid State Commun.* **84**, 639–644.

RAO, C. N. R. (1991*a*). *Chemistry of High Temperature Superconductors*. Singapore: World Scientific.

RAO, C. N. R. (1991*b*). *Philos. Trans. R. Soc. (London) Ser. A*, **336**, 595–624.

RAO, C. N. R. (1994). *Thallium-Based High Temperature Superconductors*, edited by A. M. HERMANN & J. V. YAKHMI, pp. 357–370. New York: Marcel Dekker.

RAO, C. N. R. & RAVEAU, B. (1989). *Acc. Chem Res.* **22**, 106–113.

RAO, C. N. R., GOPALAKRISHNAN, J., SANTRA, A. K. & MANIVANNAN, V. (1991). *Physica C*, **174**, 11–13.

RAO, C. N. R., NAGARAJAN, R., GANGULI, A. K., SUBBANA, G. N., GANAPATHI, L., VIJAYARAGHAVAN, R., BHAT, S. V. & RAJU, A. R. (1990). *J. Solid. State Chem.* **88**, 163–176.

RAO, C. N. R., NAGARAJAN, R., MAHESH, R., KULKARNI, G. U., AYYAPPAN, S. & SUBBANNA, G. N. (1993). *Solid State Commun.* **88**, 757–760.

RAO, C. N. R., NAGARAJAN, R., VIJAYARAGHAVAN, R., VASANTHACHARYA, N. Y., KULKARNI, G. U., RANGA RAO, G., UMARJI, A. M., SOMASUNDARAM, P., SUBBANNA, G. N., RAJU, A. R., SOOD, A. K. & CHANDRABHAS, N. (1990). *Supercond. Sci. Technol.* **3**, 242–248.

RAVEAU, B., MICHEL, C., HERVIEU, M. & GROULT, D. (1991). *Crystal Chemistry of High T_c Superconducting Copper Oxides*. Berlin: Springer-Verlag.

SANTORO, A., BEECH, F., MAREZIO, M. & CAVA, R. J. (1988). *Physica C*, **156**, 693–697.

SIEGRIST, T., ZAHURAK, S. M., MURPHY, D. W. & ROTH, R. S. (1988). *Nature*, **344**, 231–232.

SMITH, M. G., MANTHIRAM, A., ZHOU, J., GOODENOUGH, J. B. & MARKERT, J. T. (1991). *Nature*, **351**, 549–551.

SUBRAMANIAN, M. A., TORARDI, C. C., GOPALAKRISHNAN, J., GAI, P. L., CALABRESE, J. C., ASKEW, T. R., FLIPPEN, R. B. & SLEIGHT, A. W. (1988). *Science*, **242**, 249–252.

TAKANO, M., AZUMA, M., HIROI, Z., BANDO, Y. & TAKEDA, Y. (1991). *Physica C*, **176**, 441–444.

TALLON, J. L. & WILLIAMS, G. V. M. (1990). *J. Less-Common Met.* **164–165**, 70–77.

TARASCON, J. M., LE PAGE, Y., MCKINNON, W. R., RAMESH, R., EIBSCHUTZ, M., TELEPSIS, E., WANG, E. & HULL, G. W. (1990). *Physica C*, **167**, 20–34.

TOKURA, Y. & ARIMA, T. (1990). *Jpn. J. Appl. Phys.* **29**, 2388–2402.

TOKURA, Y., TAKAGI, H. & UCHIDA, S. (1989). *Nature*, **337**, 345–347.

TORARDI, C. C., PARISE, J. B., SUBRAMANIAN, M. A., GOPALAKRISHNAN, J. & SLEIGHT, A. W. (1989). *Physica C*, **157**, 115–123.

TORARDI, C. C., SUBRAMANIAN, M. A., CALABRESE, J. C., GOPALAKRISHNAN, J., MORRISSEY, K. J., ASKEW, T. R., FLIPPEN, R., CHOWDHURY, U. & SLEIGHT, A. W. (1988). *Science*, **240**, 631–634.

TORRANCE, J. B. & METZGER, R. M. (1989). *Phys. Rev. Lett.* **63**, 1515–1518.

VERWERFT, M., VAN TENDELOO, G. & AMELINCKX, S. (1988). *Physica C*, **156**, 607–615.

VIJAYARAGHAVAN, R., GANGULI, A. K., VASANTHACHARYA, N. Y., RAJUMON, M. K., KULKARNI, G. U., SANKAR, G., SARMA, D. D., SOOD, A. K., CHANDRABHAS, N. & RAO, C. N. R. (1989). *Supercond. Sci. Technol.* **2**, 195–201.

VIJAYARAGHAVAN, R., MICHEL, C., MAIGNAN, A., HERVIEU, M., MARTIN, C., RAVEAU, B. & RAO, C. N. R. (1993). *Physica C*, **206**, 81–89.

WHANGBO, M. H., KANG, D. B. & TORARDI, C. C. (1989). *Physica C*, **158**, 371–376.

WHANGBO, M. H. & TORARDI, C. C. (1991). *Acc. Chem. Res.* **24**, 127–133.

WILLIAMS, A., KWEI, G. H., VON DREELE, R. B., LARSON, A. C., RAISTRICK, I. D. & BISH, D. L. (1988). *Phys. Rev. B*, **37**, 7960–7962.

WOLFF, P. M. DE, JANSSEN, T. & JANNER, A. (1981). *Acta Cryst.* A**37**, 625–636.

XIANG, X. D., MCKERNAN, S., VAREKA, W. A., ZETTL, A., CORKILL, J. L., BARBEE, T. W. & COHEN, M. L. (1990). *Nature*, **348**, 145–147.

YOSHIZAKI, R. (1991). *Physica C*, **173**, 89–92.

ZANDERBERGEN, H. W., GROEN, W. A., MIJLHOFF, F. C., VAN TENDELOO, G. & AMELINCKX, S. (1988). *Physica C*, **156**, 325–354.

ZHANG, H., WANG, Y. Y., ZHANG, H., DRAVID, V. P., MARKS, L. D., HAN, P. D., PAYNE, D. A., RADAELLI, P. G. & JORGENSEN, J. D. (1994). *Nature*, **370**, 352–354.